Supporting Information

Fabrication and Properties of a Branched $(NH_4)_xWO_3$ Nanowire Array Film and a Porous WO_3 Nanorod Array Film

Ya Liu[†], Liang Zhao[†], Jinzhan Su[†], Mingtao Li[†], and Liejin Guo[†,‡]*

[†]International Research Center for Renewable Energy, State Key Laboratory of Multiphase Flow in Power Engineering, Xi'an Jiaotong University, Shaanxi 710049, China

[‡]The College of Engineering, Department of Mechanical Thermal Engineering and Chemical & Material Engineering, King Abdulaziz University, Jeddah 21589,Saudi Arabia

* E-mail: mingtao@mail.xjtu.edu.cn. Tel: (+86) 29-8266-8296. Fax: (+86) 29-8266-9033.

To study the branched nanowire growth process, SEM images were taken for the films with different preparation conditions, as shown in Figure S1 and S2. Figure S1 shows morphologies of FTO, seed layer, and the branched $(NH_4)_xWO_3$ nanowire array film without seed layer or glutathione. Figure S2 shows the morphologies of branched $(NH_4)_xWO_3$ nanowire array film for different growth periods.

To provide a more detailed review on the crystallization process and the chemical changes upon calcination, Figure S3-S4 display the XRD patterns and the high-resolution XPS spectra of 250 and 450 ºC annealed film. The XRD patterns indicate that, as the annealed temperature increased (< 450 ºC) the sample only exhibited small shift to the lower angle and kept the hexagonal crystal structure. The high-resolution XPS spectra indicates that the ratio of atomics N/W was reduced gradually as the annealed temperature increase, and it was near zero in the 450 ºC annealed film. While, the peaks of W^{5+} still existed the 450 ºC annealed film which indicates an existence of residual oxygen deficiency. Those results well reconfirmed the conclusions about the crystallization process and the chemical changes upon calcination.

The photo-stability test results of the porous WO_3 nanorod array film are displayed in Figure S5. The applied potential was set at 1 V vs. SCE. As illustrated in Figure S5, the photocurrent exhibited a gradual degradation, which is consistent with other studies.[1] This is because the surface of WO_x can form soluble species ($WO_3(s) + OH^{-1} \rightarrow WO_4^{2-}(aq) + H^+$) which cause the photocorrosion and can degrade the electrode material, especially in electrolyte solution with pH > 4.[2-5] Objectively speaking, for WO_3 based photoelectrode, the enhancement of photo-stability has a great significance on the applications, and requires a fair amount of researches.

The optical images and photoelectrochemical performance of the branched $(NH_4)_xWO_3$ nanowire array film before and after two months of exposure in the atmosphere are shown in

Figure S6 and S7. After two months of exposure in the atmosphere, the branched $(NH_4)_xWO_3$ still kept the original blue color. The optical and PEC test results present that the performance of the samples changed little before and after 2 months.

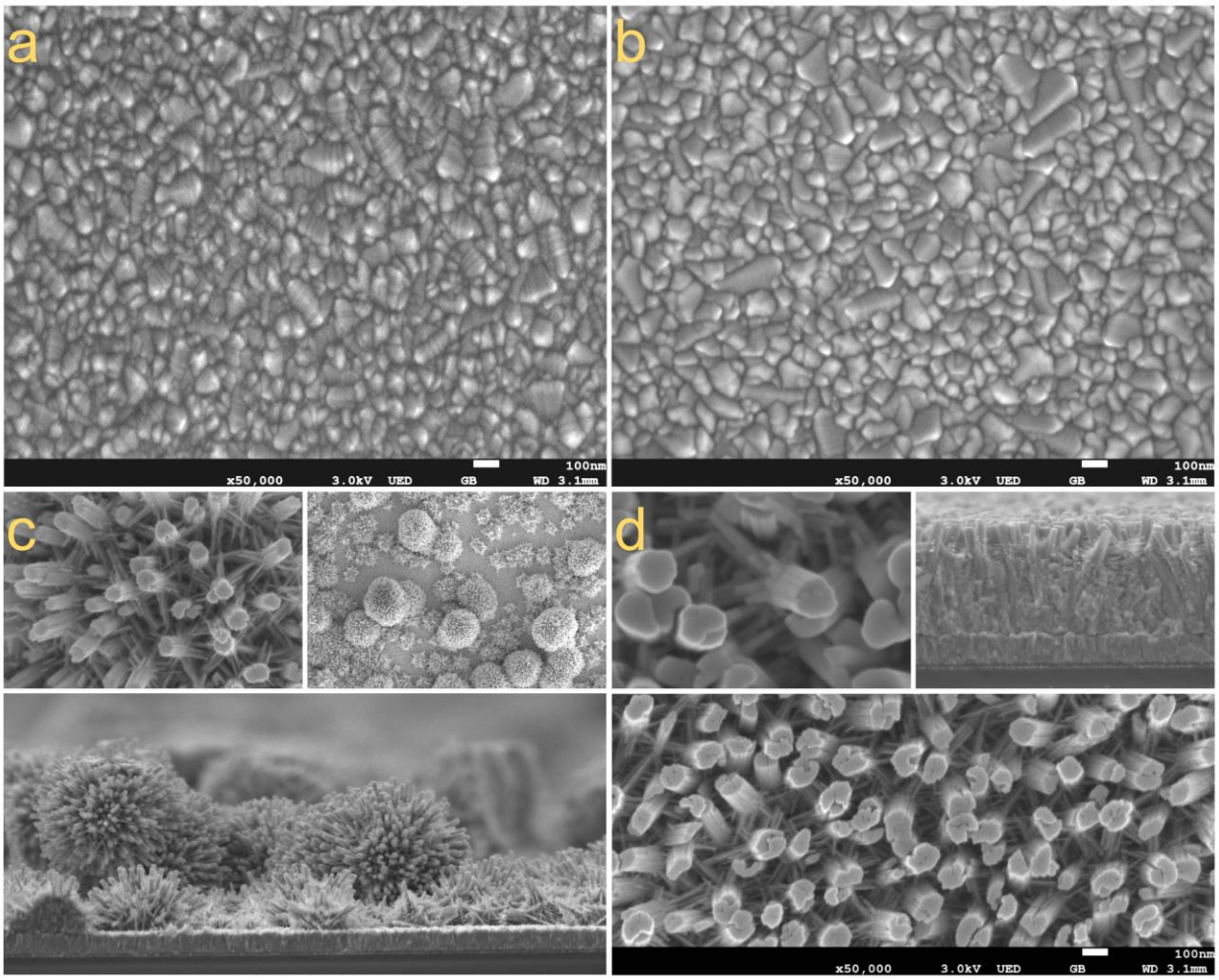

Figure S1. SEM images of (a) FTO, (b) seed layer, and the branched $(NH_4)_xWO_3$ nanowire array films (c) without seed layer or (d) L-Glutathione reduced ($C_{10}H_{17}N_3O_6S$).

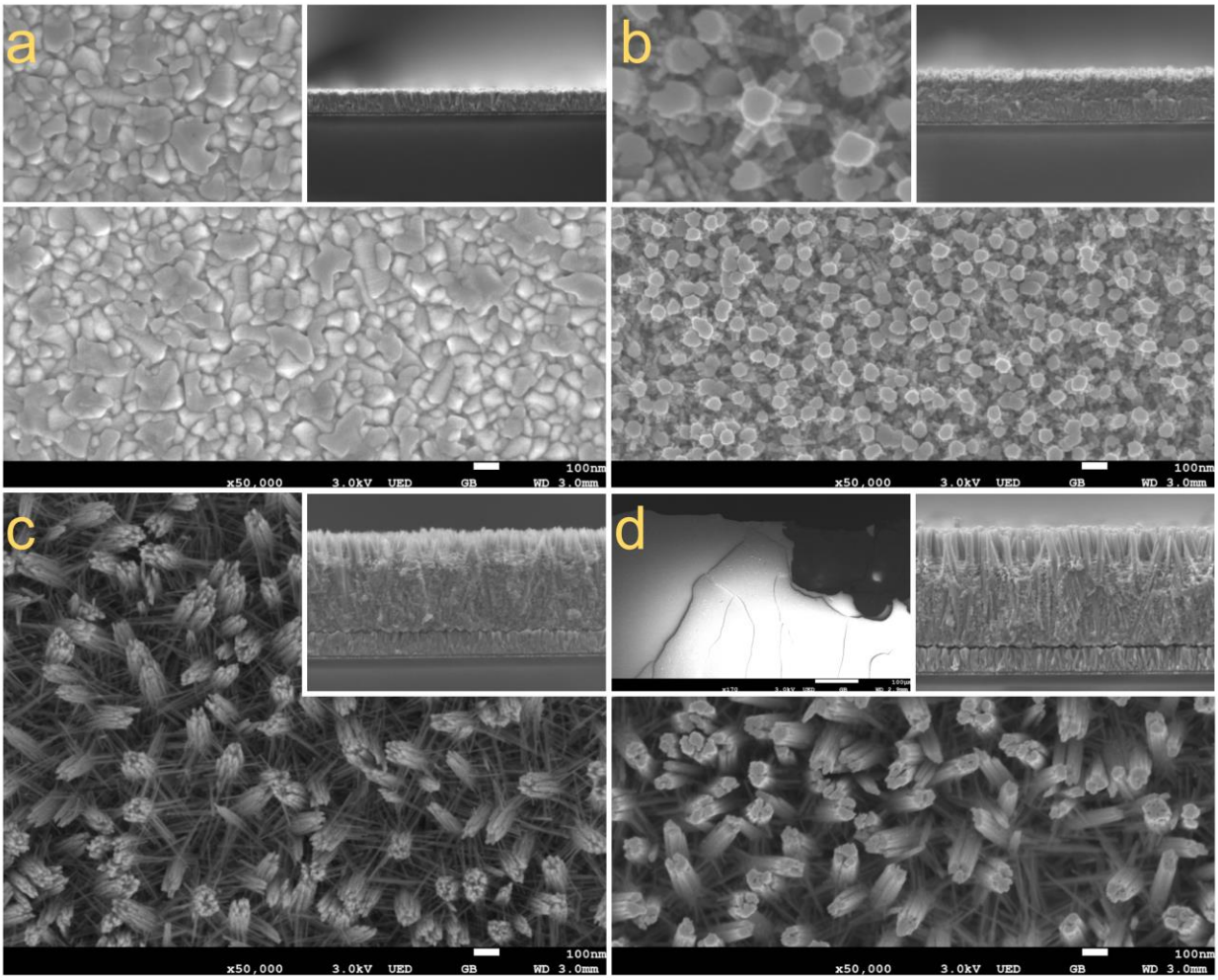

Figure S2. SEM images of the branched $(NH_4)_xWO_3$ nanowire array film for different growth times of: (a) 1 h, (b) 2 h, (c) 4 h, and (d) 8 h.

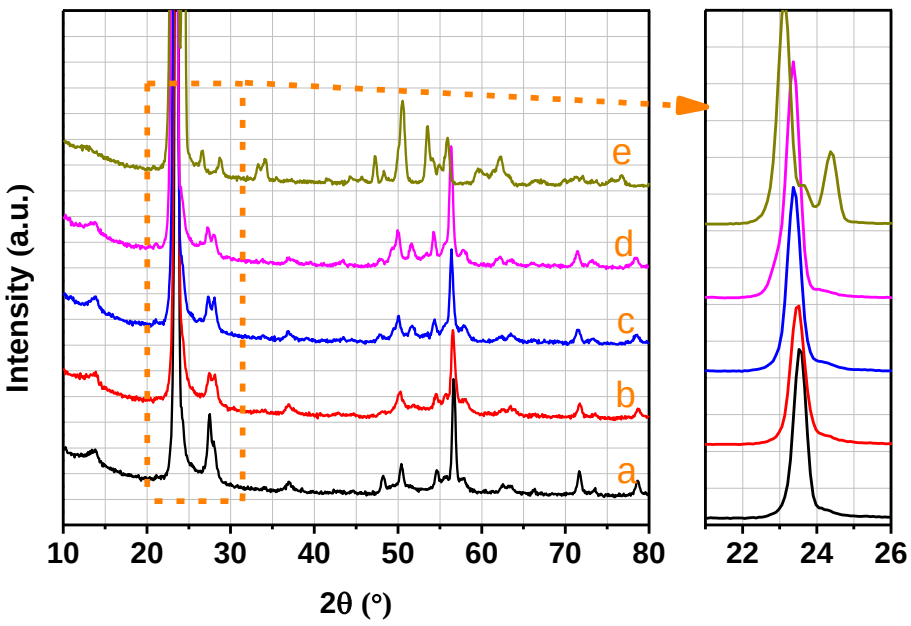

Figure S3. XRD patterns of (a) the branched $(NH_4)_xWO_3$ nanowire array film, **(b) the 250 ºC annealed film**, (c) the 350 ºC annealed film, **(d) the 450 ºC annealed film**, and (e) the 550 ºC annealed film.

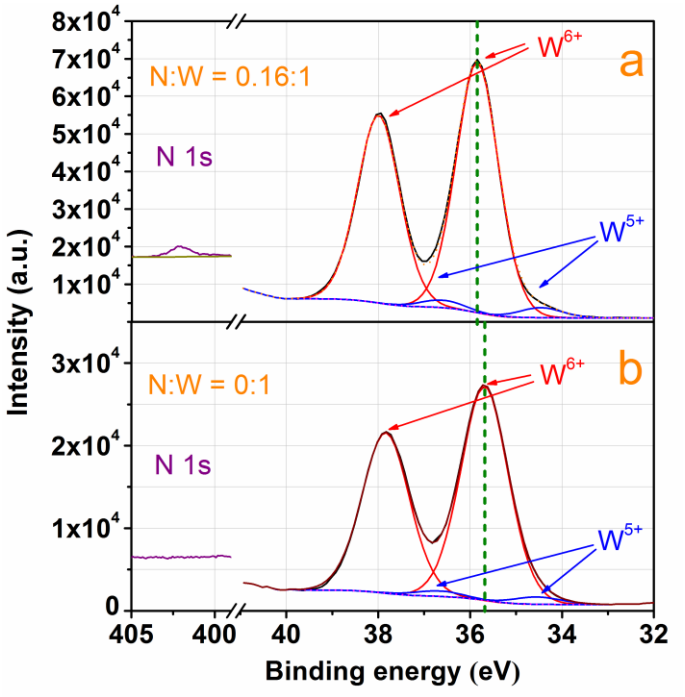

Figure S4. High-resolution XPS spectra of N 1s and W 4f for (a) the 250 ºC annealed film and (b) the 450 ºC annealed film.

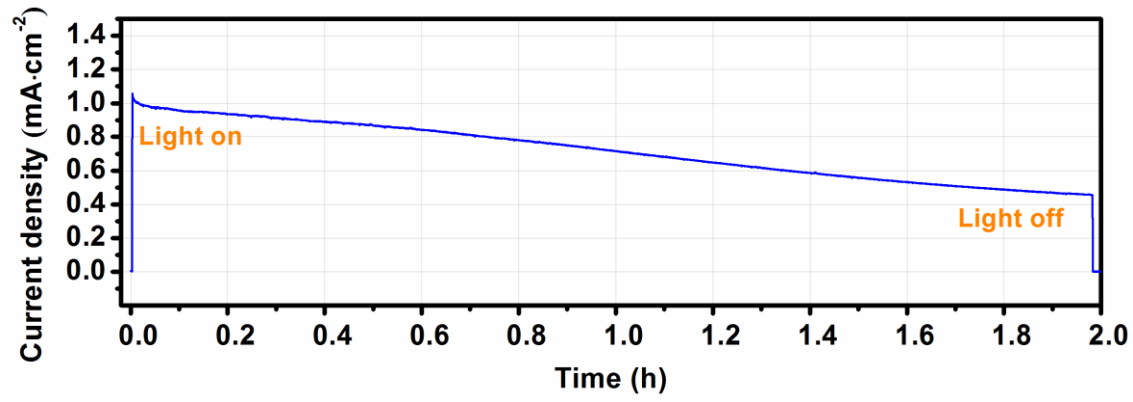

Figure S5. Current–time curves of the porous WO_3 nanorod array film.

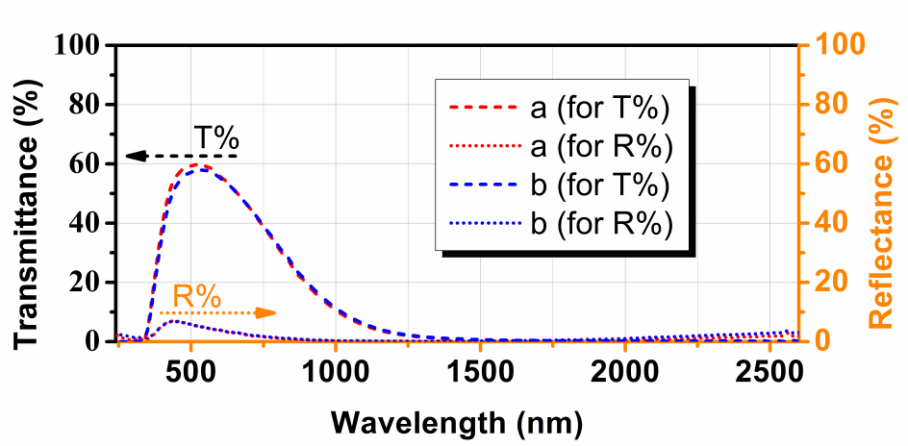

Figure S6. Optical images of (a) the fresh branched $(NH_4)_xWO_3$ nanowire array film and (b) the branched $(NH_4)_xWO_3$ nanowire array film after 2 months of exposure in the atmosphere.

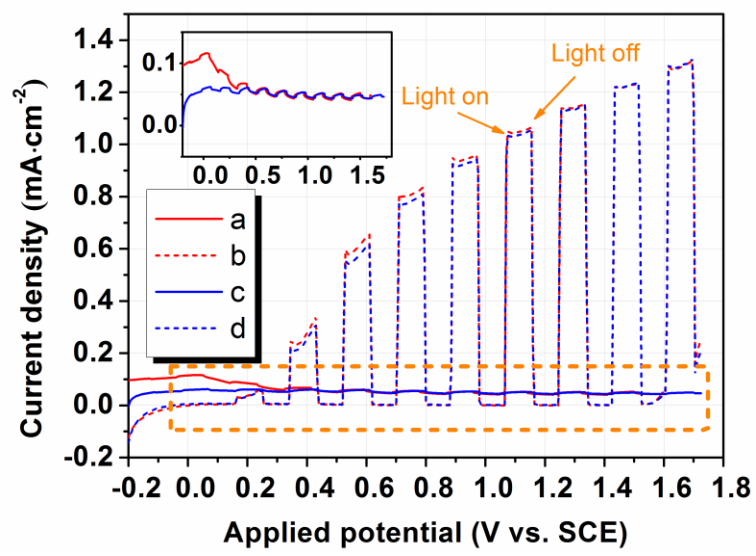

Figure S6. The photoelectrochemical performance comparison of the films. (a) The fresh branched $(NH_4)_xWO_3$ nanowire array film, (b) the branched $(NH_4)_xWO_3$ nanowire array film after two months exposure in atmosphere, (c) the fresh porous WO_3 nanorod array film, and (d) the porous WO_3 nanorod array film after 2 months of exposure in the atmosphere.

REFERENCES

(1) Hill, J. C.; Choi, K.-S., Effect of Electrolytes on the Selectivity and Stability of N-type WO_3 Photoelectrodes for Use in Solar Water Oxidation. *J. Phys. Chem. C* **2012**, 116, 7612-7620.

(2) Augustynski, J.; Solarska, R.; Hagemann, H.; Santato, C. Nanostructured Thin-Film Tungsten Trioxide Photoanodes for Solar Water and Sea-Water Splitting. *Proc. Soc. Photo-Opt. Instrum. Eng.* **2006**, 6340, U140−U148

(3) Seabold, J. A.; Choi, K.-S. Effect of a Cobalt-Based Oxygen Evolution Catalyst on the Stability and the Selectivity of Photo-Oxidation Reactions of a WO_3 Photoanode. *Chem. Mater.* **2011**, 23, 1105-1112.

(4) Liu, R.; Lin, Y.; Chou, L.-Y.; Sheehan, S. W.; He, W.; Zhang, F.; Hou, H. J. M.; Wang, D. Water Splitting by Tungsten Oxide Prepared by Atomic Layer Deposition and Decorated with an Oxygen-Evolving Catalyst. *Angew. Chem., Int. Ed.* **2011**, 50, 499-502.

(5) Wang, G.; Ling, Y.; Wang, H.; Yang, X.; Wang, C.; Zhang, J. Z.; Li, Y. Hydrogen-Treated WO_3 Nanoflakes Show Enhanced Photostability. *Energy Environ. Sci.* **2012**, 5, 6180-6187.